Fabrication of 3D Macroporous Structures of II–VI and III–V Semiconductors Using Electrochemical Deposition

ARTICLE *in* LANGMUIR · NOVEMBER 2002

Impact Factor: 4.46 · DOI: 10.1021/la020296h

Fabrication of 3D Macroporous Structures of II−VI and III−V Semiconductors Using Electrochemical Deposition

Yi-Cheng Lee, Tsung-Jung Kuo, Chih-Jung Hsu, Ya-Wen Su, and Chia-Chun Chen*

Department of Chemistry, National Taiwan Normal University, and Institute of Atomic and Molecular Sciences, Academia Sinica, Taipei 116, Taiwan

Received March 27, 2002. In Final Form: September 19, 2002

Close-packed three-dimensional (3D) arrays of silica spheres assembled on an indium tin oxide (ITO) substrate surface have been prepared using sedimentation in the solution. Both galvanostatic and potentiostatic electrochemical depositions have been tested to infiltrate six different semiconductors, ZnSe, PbSe, CdSe, CdS, CdTe, and GaAs, onto the 3D silica arrays. The detailed studies of deposition parameters such as current density, deposition time, concentrations of electrolytes, solvents, and temperatures were performed to ensure the quality of resulting semiconductor films on the arrays. Followed by the removal of the silica arrays, 3D macroporous structures made from those semiconductors were obtained, and the structures exhibited 3D periodicity and uniformity. Clear diffraction peaks at ∼1350 nm of CdSe and CdS macroporous films were observed.

Introduction

Three-dimensional (3D) macroporous materials are of importance in a wide range of applications such as separation media, catalytic surface, electrochemical sensor, and thermal insulator.[1−4] In particular, highly ordered macroporous structures consisting of semiconductors with high refractive indexes have been well-known to be photonic crystals.[5] Theoretical predictions and experimental results have indicated that the crystals possess photonic band gaps (PBG) and might be used in many technical applications such as low-loss waveguides, low-threshold laser, and optical switching elements.[6−8]

Recently, two major approaches have been widely used to build up 3D macroporous materials: chemical self-assembly and physical lithography.[9,10] One of the great advantages of the former is technically easier and cheaper for the fabrications. Mainly, the chemical self-assembly involves only three technical steps: formation of colloidal arrays on a substrate by self-assembly, sequential filling with targeting materials into the interstitial spaces between colloidal arrays, and finally removal of the colloids by chemical etching to form 3D macroporous films. It has been reported that 3D macroporous films (inverse opal) consisting of various semiconductors, metals, or polymers were constructed using self-assembly.[11−13] The synthetic colloids such as spherical silica and polystyrene latex have been employed to construct 3D close-packed arrays (opal).[14,15] The ordered arrays can then be used as templates for the infiltration of targeting materials. From the technical aspect, the infiltration is the most critical step in the fabrications of inverse opals because incomplete infiltration always results in the disruption of original ordered arrays after the etching. Recently, many techniques such as chemical vapor deposition, electrochemical depositions, sedimentation of nanoparticles, and polymerization of monomers coated on colloids have been developed for the infiltration.[16−19] Among those techniques,

* To whom the correspondence should be addressed. E-mail: t42005@cc.ntnu.edu.tw.

(1) (a) Bhave, R. R. *Inorganic Membranes: Synthesis, Characteristics and Applications*; Van Nostrand Reinhold: New York, 1991. (b) Lewandowski, K.; Murer, P.; Svec, F.; Frechet, J. M. J. *Anal. Chem.* **1998**, *70*, 1629. (c) Akolekar, D. B.; Hind, A. R.; Bhargava, S. K. *J. Colloid Interface Sci.* **1998**, *199*, 92.

(2) (a) Harold, M. P.; et al. *MRS Bull.* **1994**, *19*, 34. (b) Tanev, P. T.; Chibwe, M.; Pinnavaia, T. J. *Nature (London)* **1994**, *368*, 321. (c) Deleuze, H.; Schultze, X.; Sherrington, D. C. *Polymer* **1998**, *39*, 6109.

(3) Tierney, M. J.; Kim, H. L. *Anal. Chem.* **1993**, *65*, 3435.

(4) (a) Litovsky, E.; Shapiro, M.; Shavit, A. *J. Am. Ceram. Soc.* **1996**, *79*, 1366. (b) Seino, H.; Haba, O.; Mochizuki, A.; Yoshioka, M.; Ueda, M. *High Perform. Polym.* **1997**, *9*, 333. (c) Senkevich, J. J.; Desu, S. B. *Appl. Phys. Lett.* **1998**, *72*, 258. (d) Sedev, R.; Ivanova, R.; Kolarov, T.; Exerowa, D. *J. Dispersion Sci. Technol.* **1997**, *18*, 751.

(5) (a) Yablonovitch, E.; Leung, K. M. *Nature (London)* **1998**, *391*, 667. (b) Joannopoulous, J. D.; Meade, R. D.; Winn, J. N. *Photonic Crystals: Molding the Flow of Light*; Princeton University Press: Princeton, NJ, 1995.

(6) Lin, S.-Y.; Chow, E.; Hietala, V.; Villeneuve, P. R.; Joannopoulos, J. D. *Science* **1998**, *282*, 274.

(7) Megens, M.; Wijnhoven, J. E. G. J.; Lagendijk, A.; Vos, W. L. *Phys. Rev. A* **1999**, *59*, 4727.

(8) (a) Flaugh, P. L.; O'Donnell, S. E.; Asher, S. A. *Appl. Spectrosc.* **1984**, *38*, 847. (b) Pan, G.; Kesavamoorthy, R.; Asher, S. A. *Phys. Rev. Lett.* **1997**, *78*, 3860. (c) Fink, Y.; Winn, J. N.; Fan, S.; Chen, C.; Michel, J.; Joannopoulos, J. D.; Thomas, E. L. *Science* **1998**, *282*, 1679.

(9) See for example: Xia, Y.; et al., a special issue in *Adv. Mater.* **2001**, *13*, 369.

(10) See for example: (a) Noda, S.; Chutinan, A.; Imada, M. *Nature (London)* **2000**, *407*, 608. (b) Vogelaar, L.; Nijdam, W.; Wolferen, H. A. G. M.; de Ridder, R. M.; Segerink, F. B.; Flück, E.; Kuipers, L.; van Hulst, N. F. *Adv. Mater.* **2001**, *13*, 1551. (c) Campbell, M.; Sharp, D. N.; Harrison, M. T.; Denning, R. G.; Turberfield, A. J. *Nature (London)* **2000**, *404*, 53.

(11) (a) Müller, M.; Zentel, R.; Maka, T.; Romanov, S. G.; Torres, C. M. S. *Adv. Mater.* **2000**, *12*, 1499. (b) Braun, P. V.; Wiltzius, P. *Adv. Mater.* **2001**, *13*, 482. (c) Míguez, H.; Chomski, E.; García-Santamaría, F.; Ibisate, M.; John, S.; López, C.; Meseguer, F.; Mondia, J. P.; Ozin, G. A.; Toader, O.; van Driel, H. M. *Adv. Mater.* **2001**, *13*, 1634.

(12) (a) Jiang, P.; Cizeron, J.; Bertone, J. F.; Colvin, V. L. *J. Am. Chem. Soc.* **1999**, *121*, 7957. (b) Xu, L.; Zhou, W.; Kozlov, M. E.; Khayrullin, I. I.; Udod, I.; Zakhidov, A. A.; Baughman, R. H.; Wiley, J. B. *J. Am. Chem. Soc.* **2001**, *123*, 763.

(13) (a) Deutsch, M.; Vlasov, Y. A.; Norris, D. J. *Adv. Mater.* **2000**, *12*, 1176. (b) Jiang, P.; Hwang, K. S.; Mittleman, D. M.; Bertone, J. F.; Colvin, V. L. *J. Am. Chem. Soc.* **1999**, *121*, 11630. (c) Chen, Y.; Ford, W. T.; Materer, N. F.; Teeters, D. *J. Am. Chem. Soc.* **2000**, *122*, 10472.

(14) (a) Míguez, H.; López, C.; Meseguer, F.; Blanco, A.; Vázquez, L.; Mayoral, R.; Ocaña, M.; Fornés, V.; Mifsud, A. *Appl. Phys. Lett.* **1997**, *71*, 1148. (b) Vlasov, Y. A.; Bo, J. X.- Z.; Sturm, C.; Norris, D. J. *Nature (London)* **2001**, *414*, 289. (c) Blanco, A.; Chomsld, E.; Grabtchak, S.; Ibisate, M.; John, S.; Leonard, S. W.; Lopez, C.; Meseguer, F.; Miguez, H.; Mondia, J. P.; Ozin, G. A.; Toader, O.; van Driel, H. M. *Nature (London)* **2000**, *405*, 437.

(15) (a) Gates, B.; Xia, Y. *Adv. Mater.* **2000**, *12*, 1329. (b) Miguez, H.; Meseguer, F.; López, C.; Blanco, A.; Moya, J. S.; Requena, J.; Mifsud, A. A.; Fornés, V. *Adv. Mater.* **1998**, *10*, 480. (c) Mayers, B. T.; Gates, B.; Xia, Y. *Adv. Mater.* **2000**, *12*, 1629.

10.1021/la020296h CCC: $22.00
Published on Web 11/09/2002

electrochemical deposition provides a relatively efficient and safe route for the infiltration. In particular, there is less toxic or volatile raw material involved for the depositions of binary II−VI and III−V semiconductors.

The 3D macroporous structures of CdSe and CdS semiconductors have been prepared using the technique based on both self-assembly and electrochemical depositions.[11b] The physical properties of those structures have been also investigated. However, most previous studies mainly focused on the optical applications of resulting macroporous structures, but not on the experimental details of electrochemical depositions. Because the fundamental electrochemical characteristics of semiconductor ions are quite different, their deposition conditions might be varied significantly. Thus, there still remain many technical challenges of applying electrochemical depositions to entirely infiltrate various II−VI and III−V semiconductors onto silica colloidal arrays and then to prepare 3D macroporous structures with desired quality. In particular, there is still no report on the fabrications of 3D macroporous structures of the high refractive index semiconductor, GaAs, using electrochemical deposition.

In this paper, we prepare close-packed colloidal arrays of 0.5 μm silica assembled on an indium tin oxide (ITO) substrate surface using sedimentation. Both galvanostatic and cyclic potentiostatic electrochemical depositions are tested individually to infiltrate various semiconductors onto the arrays, and the studies on detailed deposition parameters such as current density, deposition time, concentrations of electrolytes, solvents, and temperatures are discussed. We are able to fabricate the films of six different semiconductors, ZnSe, PbSe, CdSe, CdS, CdTe, and GaAs, onto the silica arrays. Following by the removal of silica arrays, 3D macroporous structures made from those semiconductors are built, and their optical properties are measured.

Experimental Section

Preparation of Silica Sphere Arrays. Monodisperse silica colloids were either obtained from Lancaster Chemicals or prepared by a sol−gel method according to a previous report.[20] Typically, spherical silica colloids of ~1.5 g with 0.5 μm in diameter were dispersed into ethanol of 100 mL in a flask. A glass slide (1.5 × 0.5 cm^2) coated with indium tin oxide (ITO) was placed on the bottom of the vial. Through self-assembly of the silica colloids, 3D colloidal templates were formed within 7−10 days while ethanol was evaporated slowly. By adjusting the amount of silica in ethanol, the thickness of the resulting templates (50−100 μm) can be precisely controlled.

Electrochemical Depositions. All solutions and chemicals were used as received. Notice that most of starting materials such as SeO_2 and As_2O_3 are highly toxic and should be handled with adequate precautions. Two different deposition techniques were applied to grow semiconductor films onto silica arrays. Galvanostatic deposition was performed onto the colloidal template using a dc power supply (Keithley 2400). Potentiostatic deposition was carried on an electrochemical analyzer operated in cyclic voltammetry (CV) mode (PARC EG&G, model 273) with a conventional three-electrode setup, using a saturated calomel reference electrode (SCE). The detailed chemistry of both deposition techniques is described below. In a typical reaction for the potentiostatic deposition of CdSe, the electrolytes contained 0.3 M $CdSO_4$, 0.25 M H_2SO_4, and 0.7 mM SeO_2. The solutions were prepared using 18 MΩ deionized water. The potential was cycled between −400 and −800 mV vs SCE at a scan rate of 0.75−16 V/s.

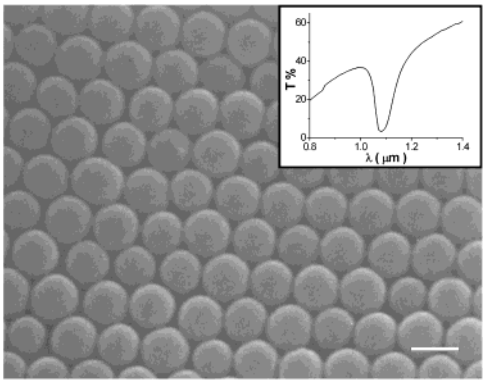

Figure 1. Typical scanning electron micrograph (SEM) image of an ordered array made from 0.5 μm silica spheres. The top surface is a (111) plane of an fcc structure. The transmission spectrum of the sample (inset) was measured at normal incidence ($\theta = 0°$). A clear attenuation band in the spectrum is observed due to Bragg diffraction related to the (111) planes. The scale bar is 500 nm.

Fabrication of 3D Macroporous Structures. At the beginning of the depositions, generally the templates showed clear visible colors from semiconductor films. In the galvanostatic deposition, a thick layer (more than micrometer) of semiconductor film was obtained within a few minutes. In the cyclic potantiostatic deposition, semiconductor films tenths or hundredths of nanometers in thickness can be observed after a few cycles. Depending on the thickness of the colloidal template, careful adjustments on the experimental parameters were performed to achieve complete infiltration of the interstitial spaces of silica spheres. Following electrochemical deposition, the template was dissolved with an aqueous 5.5% HF solution for 20−30 min to remove the silica spheres. The resulting 3D macroporous arrays were dried under vacuum.

Sample Characterization. A JEOL scanning electron microscopy (SEM) and energy-dispersive X-ray spectroscopy were used to characterize 3D colloidal arrays and macroporous structures. A sputter system was executed to deposit a thin layer (1−3 nm) of gold on the samples before SEM measurements. The crystal structures of resulting semiconductor films after the deposition were confirmed using a powder X-ray diffractometer (Toshiba, A-40-Cu). Transmission spectra are obtained using an UV−near-IR spectrometer (Perkin-Elmer, λ-900).

Result and Discussion

Preparations of Silica Spheres Arrays. Figure 1 shows a typical SEM image of the ordered arrays made of 0.5 μm silica spheres on an ITO substrate surface. The image clearly exhibits a 3D crystalline order with an fcc close-packing structure with the (111) planes along the substrate. The ordered structure has a long-range order up to 1 cm in a larger scale image and consists of more than hundreds of layers of silica spheres. The opaline ordered arrays exhibit good optical quality. The transmission spectrum (inset in Figure 1) shows a stop band at the peak position of 1080 nm. This value is in agreement with the data obtained from previous experimental observations[14a,15b] and theoretical calculations on the basis of Bragg's law. The optical property of the arrays provides additional evidence of their 3D periodicity and uniformity. Thus, the 3D silica arrays assembled on ITO substrates can be used as the templates for the electrochemical depositions of various semiconductors.

Electrochemical Deposition of Semiconductor Films. Electrochemical depositions offer several advantages in the preparations of semiconductor thin films onto silica arrays.[21] In particular, because the depositions are

(16) (a) Yang, P.; Rizvi, A. H.; Messer, B.; Chmelka, B. F.; Whitesides, G. M.; Stucky, G. D. *Adv. Mater.* **2001**, *13*, 427. (b) Chomski, E.; Ozin, G. A. *Adv. Mater.* **2000**, *12*, 1071.
(17) Braun, P. V.; Wiltzius, P. *Nature (London)* **1999**, *402*, 603.
(18) Vlasov, Y. A.; Yao, N.; Norris, D. J. *Adv. Mater.* **1999**, *11*, 165.
(19) Míguez, H.; Meseguer, F.; López, C.; López-Tejeira, F.; Sánchez-Dehesa, J. *Adv. Mater.* **2001**, *13*, 393.
(20) Stober, W.; Fink, A.; Bohn, E. *J. Colloid Interface Sci.* **1968**, *26*, 62.

Table 1. Experimental Parameters of Electrochemical Depositions of Different Semiconductors

material	electrolyte	solvent[a]	temp (°C)	current density (mA/cm^2)	deposition time (min)
CdTe	2.0×10^{-2} M Te 6.0×10^{-2} M TBP 4.0×10^{-3} M $Cd(ClO_4)_2$ 1.0×10^{-1} M $LiClO_4$	DMSO	100	3	4
GaAs	7.5×10^{-1} M $Ga(NO_3)_3 \cdot xH_2O$ 5.0×10^{-2} M As_2O_3	DI	25	2	4
CdS	1.9×10^{-2} M S 5.5×10^{-1} M $CdCl_2$	DMSO	120	2	4
CdSe	3.0×10^{-3} M SeO_2 3.0×10^{-1} M $CdSO_4$	DI	25	2	5
PbSe	5.0×10^{-2} M $Pb(NO_3)_2$ 1.0×10^{-3} M SeO_2	DI	25	2	5
ZnSe	5.0×10^{-4} M SeO_2 2.0×10^{-1} M $ZnSO_4 \cdot 7H_2O$ 2.0×10^{-1} M K_2SO_4	DI	25	3	5

[a] DMSO = dimethyl sulfoxide; DI = deionized water.

performed in a solution phase, they provide an efficient route to achieve entire infiltration of semiconductors onto the interstitial spaces between 3D silica arrays. In addition, the quality of semiconductor films can be controlled by the careful adjustments on experimental parameters during the depositions.[22−24] In this work, galvanostatic and potentiostatic electrochemical depositions have been used to infiltrate II−VI and III−V semiconductor film onto silica arrays. The detailed studies on the experimental conditions of both methods are summarized as the following.

Galvanostatic Electrochemical Depositions. We have tested several important parameters independently to ensure successful depositions of each semiconductor films according to previous reports.[21−24] Table 1 lists the optimized conditions of galvanostatic depositions of six different semiconductors onto the arrays. The significant effects of each parameter in the table are discussed as the following. **(**A**)** The concentrations of electrolytes were initially estimated on the basis of Faraday's law and the desired thickness of resulting films. The relative concentrations of electrolytes were adjusted to reach a right stoichiometry of resulting films. For example, the ratio of $[CdSO_4]/[SeO_2] = 100$ was found for the successful formation of CdSe films. Lowering the ratio (increasing $[SeO_2]$) resulted in the formation of CdSe films with excess selenium on the surface. **(**B**)** The deposition temperatures were related to the solvents used and the solubility of different electrolytes. Here, deionized water and dimethyl sulfoxide (DMSO) were applied to dissolve strong electrolytes and pure elements, respectively. Typically, for the depositions of CdS and CdTe films, the solution was kept at the temperature of 110−120 °C to ensure complete dissolving of elemental sulfur and tellurium in DMSO. **(**C**)** Both the thickness and smoothness of the film surface were mainly controlled by the current density and the deposition time. Under the conditions that the current density of 1−3 mA/cm^2 was applied and the deposition time was around 5 min, the resulting films with the thickness of ∼10 μm were observed. However, a lower current density and a longer deposition time were not a general rule to obtain a more uniform surface and thicker films as described below. **(**D**)** The sizes of polycrystals of resulting semiconductor films were mainly determined by the current density applied.[21b] When the applied current density was too low (<1 mA/cm^2 in our experiments), the resulting particle sizes were so large that most of the interstitial spaces between colloids were blocked, and thus unsuccessful deposition was often found. On the other hand, when the applied current density was too high (>3 mA/cm^2), the growth of semiconductor films was too fast. As a result, the uniformity of the film thickness became very poor. In our samples, effective depositions occurred when the current density was controlled within the range of 1−3 mA/cm^2. **(**E**)** The thickness of as-grown semiconductor films should be underlying the silica layers after the depositions. If the entirely ordered arrays were completely embedded by semiconductor films, the removal of silica spheres by HF solution became difficult.

Potentiostatic Electrochemical Depositions. For the deposition of those six semiconductor films above using potentiostatic electrochemical deposition, the applied potentials, electrolytes, and scan rates were varied for each case. Overall, the molar ratio of electrolytes and scan rate were two key factors determining the quality of all resulting semiconductor films and their stoichiometry. The semiconductor films with tenths or hundredths of nanometers in thickness were obtained after a few cycles. However, although we have tested various experimental conditions, there were still some difficulties for the depositions of semiconductor thin films onto silica arrays using potentiostatic electrochemical deposition. A serious problem here was that the silica arrays on ITO substrate was easily falling apart after a layer of few hundred nanometer films was deposited. On the basis of previous observations,[24] we speculated that at the beginning of the deposition most of the materials on the substrate consisted of both semiconductor film (i.e., CdSe, PbSe) and excess metal (i.e., Cd, Pb). After the deposition was continued for several cycles, the excess metal either reacted with free counter element (Se) to form a semiconductor film or was reduced off to the solution by a positive potential. During the reduction process, the adhesion of excess metal and silica surface could be very poor and then cause the falling apart of all the materials away from the substrate. In most cases, we found that the experiments for the formation of thick semiconductor films onto the arrays

(21) (a) Edamura, T.; Muto, J. *Thin Solid Films* **1993**, *235*, 198. (b) Yang, M.-C.; Landau, U.; Angus, J. C. *J. Electrochem. Soc.* **1992**, *139*, 3480. (c) Klein, J. D.; Herrick, I. R. D.; Palmer, D.; Sailor, M. J.; Brumlik, C. J.; Martin, C. R. *Chem. Mater.* **1993**, *5*, 902. (d) Streltsov, E. A.; Osipovich, N. P.; Ivashkevich, L. S.; Lyakhov, A. S.; Sviridov, V. V. *Electrochim. Acta* **1998**, *43*, 869.

(22) (a) Gao, Y.; Han, A.; Lin, Y.; Zhao, Y.; Zhang, J. *J. Appl. Phys.* **1994**, *75*, 549. (b) Mastai, Y.; Hodes, G. *J. Phys. Chem. B* **1997**, *101*, 2685.

(23) (a) Wade, T. L.; Ward, L. C.; Maddox, C. B.; Happek, U.; Stickney, L. *Electron. Solid State Lett.* **1999**, *2*, 616. (b) Sahu, S. N. *J. Mater. Sci. Mater Electron.* **1992**, *3*, 102. (c) Cuomo, J. J.; Gambino, R. J. *J. Electrochem. Soc.* **1968**, *115*, 755.

(24) Kressin, A. M.; Doan, V. V.; Klein, J. D.; Sailor, M. J. *Chem. Mater.* **1991**, *3*, 1015.

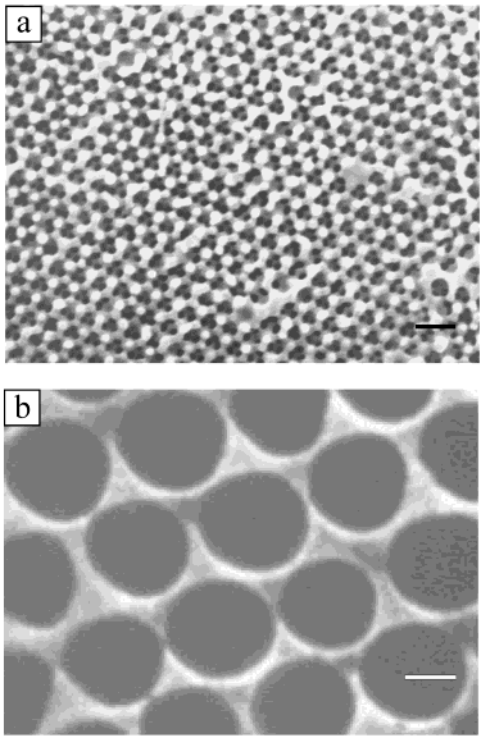

Figure 2. (a) Typical SEM top view images of deposited CdSe film after removal of 0.5 μm silica spheres. The image shows a periodically macroporous structure. The scale bar is 1 μm. (b) High magnification view of SEM image clearly showing the contact points between each holes were constructed firmly. The scale bar is 250 nm.

were not quite successful using potentiostatic deposition since a thick layer of semiconductor film cannot be reached.

In comparison to galvanostatic electrochemical depositions, potentiostatic deposition might provide a better control, in principle, of the stoichiometry of resulting semiconductor films. However, the galvanostatic deposition was more suitable to apply for the formation of a semiconductor film with the thickness up to more than 10 μm on silica arrays, and also the quality of the film was much easier controlled through the adjustments of experimental parameters.

Fabrications of Macroporous Structures. The 3D macroporous structures were fabricated after the template was immersed in HF solution. The samples were first characterized using scanning electron microscopy (SEM) with the attachment of energy-dispersive X-ray spectroscopy (EDXS) to measure their stoichiometry and surface morphology. The molar ratios of the cation/anion of the II−V semiconductors were found to be ≈1 for all successful depositions on the basis of EDXS measurements (see below for III−V semiconductors). In addition, an X-ray powder diffractometer was applied to confirm the structures of each semiconductor film. Figure 2 shows typical SEM images of deposited CdSe film after removal of silica spheres. This film exhibits 3D periodicity and uniformity macroporous structure over a long range (Figure 2a). The structure is constructed at contact points between the original silica arrays, and their arrangement on a triangular lattice indicates that the macroporous structures are a hexagonal close-packed array. In particular, the image in Figure 2b shows that the contact points between each hole are constructed firmly. The image suggests that the interstitial spaces of silica arrays are entirely filled with semiconductors by the electrochemical depositions in the solution. Holes into the layer below in Figure 2a are

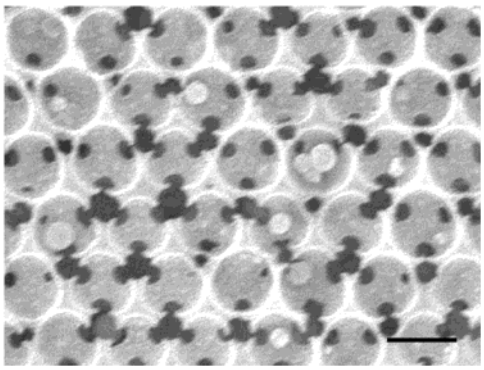

Figure 3. Typical SEM image shows the periodical macroporous structure of GaAs film. The scale bar is 500 nm.

clearly observed, indicating the 3D nature of the structures. The average diameter of the holes (∼0.5 μm) is close to that of the silica spheres of the template. The result suggests that there is no significant contraction or expansion of the macroporous structure after removal of silica, and the silica template is completely dissolved in HF solution without any degradation of the structure. However, after HF etching, the disruptions of semiconductor macroporous structures were observed occasionally in SEM images. The disruptions were probably due to either poor crystallinity of as-grown semiconductor films or weak adhesion between ITO substrate and semiconductor polycrystals or between polycrystals themselves. The poor crystallinity of the films can be improved by the annealing at 300−500 °C under vacuum depending on the types of semiconductors.

Electrochemical Depositions of III−V Semiconductors. The depositions of III−V semiconductor films onto silica sphere arrays were much more difficult to achieve than those of II−VI semiconductor mainly because of more covalent (less ionic) characteristic of the former than that of the latter. Figure 3 shows the SEM images of 3D macroporous structures of GaAs semiconductors. The film exhibits shinning black color and has 3D periodical and uniform macroporous structure in a long range similar to the structures shown in Figure 2. The formation of GaAs film was also confirmed using EDXS spectroscopy. During the deposition, we found that the most critical parameter to obtain good quality of GaAs film was the control of the ratio of the electrolytes, $[Ga(NO_3)_3]/[As_2O_3]$. The ratio of much higher than 1 was always necessary to achieve the film formation (Table 1). Lowering the ratio resulted in the formation of arsenic oxide and pure arsenic on the basis of XRD measurements. However, a small amount of arsenic oxide was still detected in most of our samples. Also, the quality of the GaAs macroporous film in terms of their uniformity and crystallinity was not as good as that of the II−V semiconductors reported in this work. Thus, further optimizations on the experimental conditions were still required to increase the crystallinity of GaAs macroporous film.

The fabrications of other III−V semiconductor macroporous films of InP, InAs, and GaP failed in our experiments, although several different electrolytes and experimental parameters have been intensively tried during the electrochemical deposition step. Overall, the failure was mainly attributed to the poor conductivity of ITO glass because of the strong acidity of electrolytic solutions we used according to the previous reports.[23] For the electrochemical deposition of those III−V semiconductors, it remains a challenging work to find a proper deposition condition and to preciously control the ratio of cation and

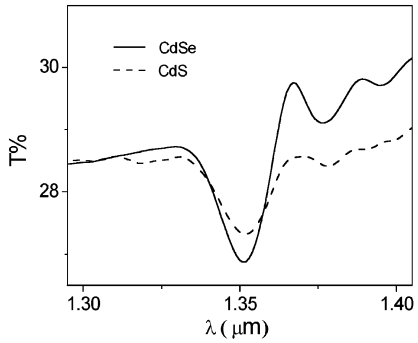

Figure 4. Optical transmission spectra of CdSe and CdS 3D macroporous structures measured at normal incidence (θ = 0°). The diffraction peaks of CdSe and CdS curves are clearly observed at the positions of λ = 1350 and 1352 nm, respectively.

anion of the resulting films. In the future, possible methods such as molten salt of those semiconductors at high temperatures might be tried for the depositions.

Optical Properties of Macroporous Structures. Theoretical calculations[5] on photonic band structures have indicated that 3D macroporous semiconductor films require to have high refractive indexes, excellent periodicity, and uniformity to obtain a PBG. Because of the periodicity and uniformity of the 3D macroporous semiconductor films over a long range, our samples of II−V semiconductors demonstrate interesting optical properties. Figure 4 shows the transmission spectra of the films of CdSe and CdS. The spectra clearly show the diffraction peaks at the positions of 1350 and 1352 nm. The peaks can also be theoretically calculated from Bragg's law. At normal incidence, the spectral position of the absorption peak can be derived from $\lambda = 2n_{\text{eff}}d_{111}$, where n_{eff} is the average refractive index of the semiconductor films at optical frequencies and d_{111} is the interlayer spacing of the air spheres along the (111) direction. This spacing is related to the sphere diameter D by $d_{111} = (2/3)^{1/2}D$ for any close-packed structure. The diffraction peak of ~1465 nm for both CdSe and CdS is obtained based on the theoretical calculations, when both semiconductor matrixes with refractive index of 2.5−2.6 and D = 500 nm are introduced.[25] Most likely, the differences between experimental and theoretical values are attributed to the uncertainty of the refractive indexes of CdSe and CdS under the condition that the macroporous films are not perfect crystals. In the other way, a pore diameter (D) of 460 nm is obtained, if the experimental value of 1350 nm is introduced into the equation above. However, we think that the latter case is less likely because there is no residual silica left behind after the etching based on their SEM images. In the future, further theoretical calculations and experiments should be performed to address more detailed optical properties of semiconductor macroporous structures.

In conclusion, the electrochemical depositions of six different semiconductor films onto ordered silica arrays have been successfully made. Systematic studies on their experimental parameters were performed during the depositions. The 3D macroporous structures of those semiconductors were built by the removal of silica spheres. The resulting semiconductor macroporous structures exhibited 3D periodicity and uniformity. The CdSe and CdS macroporous films showed clear diffraction peaks at around 1350 nm.

Acknowledgment. This work was supported by the National Science Council, Chinese Petroleum Cooperation, and National Taiwan Normal University (ORD-91-01). We thank Profs. K.-J. Ma, Y.-F. Chen, C.-N. Chang, H.-E. Horng, H.-L. Liu, C.-C. Yang, L.-C. Chen, and Dr. K.-H. Chen for comments on this manuscript and help with electron microscopy measurements.

LA020296H

(25) Norris, D. J.; Vlasov, Y. A. *Adv. Mater.* **2001**, *13*, 371.